

Supporting Information:

Gold-Copper Nanoparticles: Nanostructural Evolution and Bifunctional Catalytic Sites

Jun Yin,^a Shiyao Shan,^a Lefu Yang,^{a,b} Derrick Mott,^{a,†} Oana Malis,^c Valeri Petkov,^d Fan Cai,^b Mei Shan Ng,^a Jin Luo,^a Bing H. Chen,^b Mark Engelhard,^c and Chuan-Jian Zhong^{*a}

^a Department of Chemistry, State University of New York at Binghamton, Binghamton, NY, 13902, USA.

^b College of Chemistry and Chemical Engineering, Xiamen University, Xiamen 361005, China.

^c Physics Department, Purdue University, West Lafayette, IN 47907, USA.

^d Department of Physics, Central Michigan University, Mount Pleasant, MI 48859, USA

^e EMSL, Pacific Northwest National Laboratory, Richland, Washington 99352, USA

* E-mail: cjzhong@binghamton.edu

† Present address: School of Materials Science, Japan Advanced Institute of Science and Technology, 1-1 Asahidai, Nomi, 923-1292 Ishikawa, Japan.

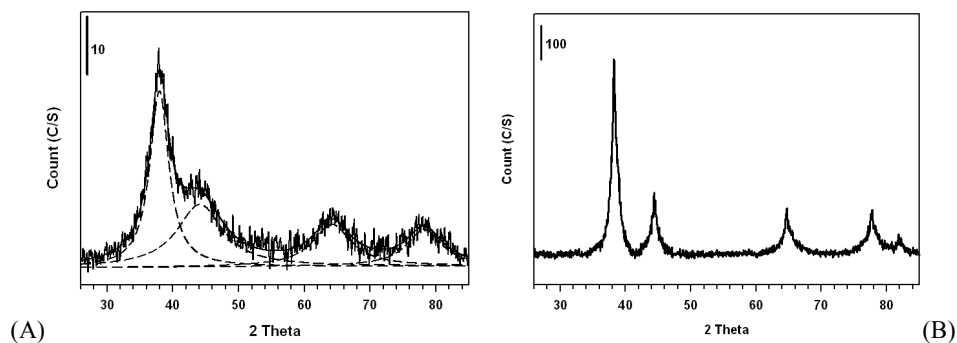


Figure S1. XRD pattern for a sample of as-synthesized Au₂₅Cu₇₅ nanoparticles (A) and a sample of as-synthesized Au₅₀Cu₅₀ nanoparticles after a thermal treatment at 156 °C for 3 hr.

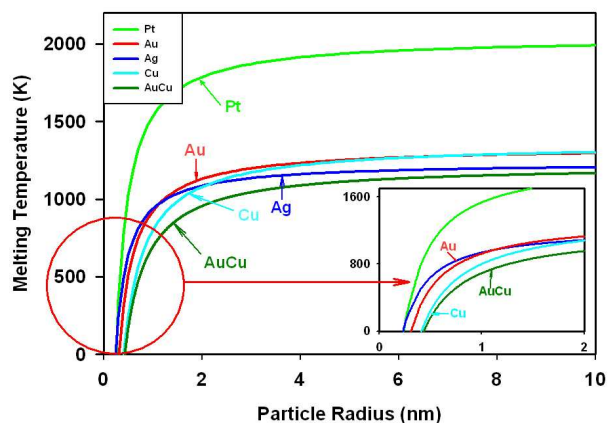


Figure S2. Theoretical melting curves for Au, Cu, Ag, and Pt particles as a function of particle radius (r) (The parameters used in the calculation are shown in Table S1. The theoretical melting curves calculated for different metal particles as a function of particle sizes (r -radius) are derived the thermodynamic model^[2]. Theoretically, melting curves of nanosized Au, Cu, Ag, and Pt can be calculated as a function of the particle sizes (r - radius) based on a thermodynamic model as follows,

$$\frac{T_r - T_\infty}{T_\infty} = -\frac{4}{\rho_s L 2r} \left[\gamma_s - \gamma_l \left(\frac{\rho_s}{\rho_l} \right)^{2/3} \right] \quad (1)$$

where T_r and T_∞ are melting temperatures of the particle and the bulk solid, respectively, r is the radius of the particle, ρ_s and ρ_l are the density of the respective solid and the liquid phases, γ_s and γ_l are the surface energy of the solid and the liquid, and L is the heat of fusion. The theoretical model predicts a decrease of the melting point with decreasing particle radius (r). The solid-like behavior of nanoparticles can be illustrated by comparing the theoretical melting curves for Au, Cu, Ag, and Pt as a function of particle sizes (r -radius)^[1,2] (S.I. Fig. S2, Table S1). For nanoparticles smaller than 2 nm in diameter, the theoretical melting temperatures (T_r), are much lower than their bulk ones, exhibiting T_r (Cu) < (Au) ~ (Ag) << (Pt). The surface melting temperature could be significantly lower at $r < 2$ nm than the theoretical ones^[2], as found by studying the thermal evolution of Au nanoparticles^[1,3]. and thiolate-capped Cu nanoclusters to Cu₂S nanodiscs^[4].

Table S1. Physical parameters used in the calculation of melting curves

	ρ_s (kg/m ³)	ρ_L (kg/m ³)	T_∞ (K)	L (J/kg)	γ_s (J/m ²)	γ_L (J/m ²)
Au	19000 ^[2]	17280 ^[2]	1337 ^[2]	63384 ^[2]	1.4 ^[5]	1.14 ^[5]
Cu	8960 ^[2]	8020 ^[2]	1358 ^[2]	207187.5 ^[2]	1.78 ^[5]	1.3 ^[5]
Ag	10490 ^[2]	9320 ^[2]	1235 ^[2]	104444 ^[2]	1.1 ^[5]	0.895 ^[5]
Pt	21450 ^[2]	19770 ^[2]	2041 ^[2]	112538 ^[2]	2.2 ^[5]	1.8 ^[5]
Au ₃ Cu	17110 ^a	15510 ^a	1220 ^[6]	77698 ^a	1.59 ^b	1.22 ^b

Note: a) calculated based on the bimetallic composition and the data from the monometallic compositions; b) calculated based an average between the monometallic data.

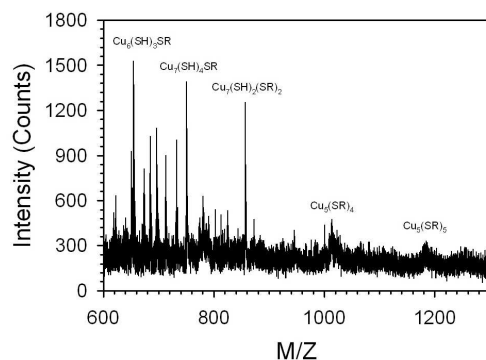


Figure S3. Maldi-Tof mass spectrum for as-synthesized thiolate-capped copper nanoclusters. The spectrum was collected with an Ettan instrument from GE Healthcare operated in reflection mode with

the accelerating voltage held constant at 20 kV. The calibration standards used were proteins of molecular weight 1046.54 and 2464.91. The matrix used for samples was DCTB, while that used for calibrants was sinapinic acid. The spectrum in Figure S3 was collected for a sample prepared by TLC separation of the nanoclusters from a solution. The matrix used for the sample was DCTB (*trans*-2-[3-(4-*tert*-butylphenyl)-2-methyl-2-propenylidene]-malononitrile).

Table S2. Primary peaks identified from the Maldi-Tof spectrum, and the possible structures and masses. For this sample of nanoparticles, peaks in the region of 600 ~ 1200 (m/z) were detected. Preliminary analysis of the peak positions for the significant peaks, along with calculated masses for the associated clusters, seemed to suggest the presence of Cu₅₋₇ clusters such as Cu₅(SR)₄, Cu₅(SR)₅, Cu₆(SH)₃SR, Cu₇(SH)₄SR, and Cu₇(SH)₂(SR)₂.

Peak Position (Primary Peak)	Possible Structure	Calculated Mass
655.11	Cu ₆ (SH) ₃ SR	653.77
750.99	Cu ₇ (SH) ₄ SR	750.38
857.01	Cu ₇ (SH) ₂ (SR) ₂	857.58
1013.77	Cu ₅ (SR) ₄	1011.02
1185.01	Cu ₅ (SR) ₅	1184.35

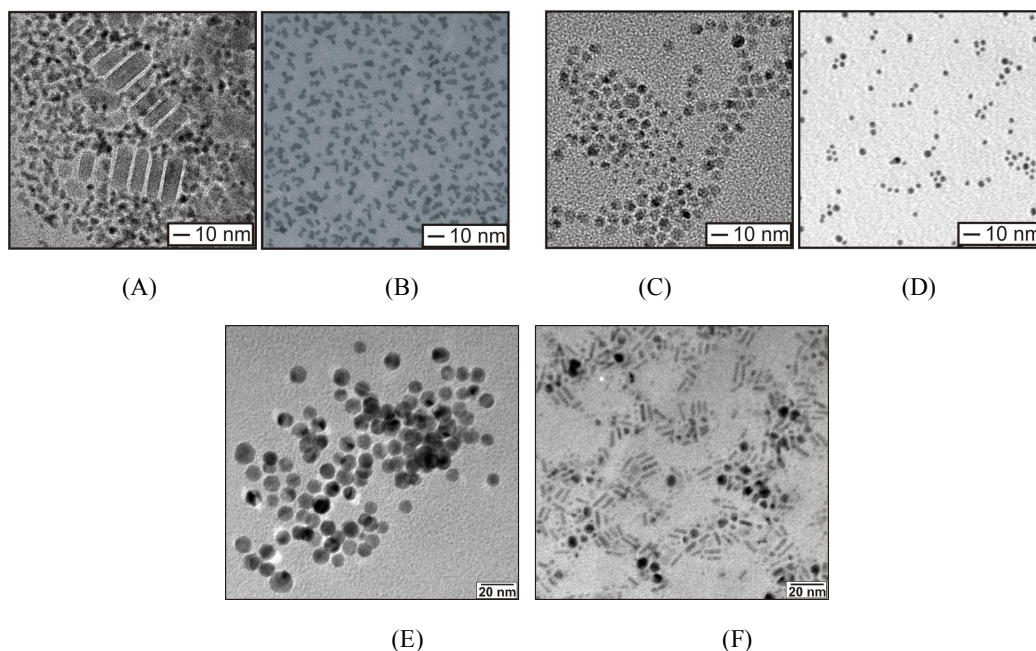


Figure S4. TEM micrographs for samples from binary solutions of Cu + Pt and Cu + Ag nanoparticle systems. (A) a sample from heating a binary solution of Cu nanoclusters and Pt nanoparticles ($T=220$ °C, $t_h=1.5$ hr); (B) Pt nanoparticles; (C) a sample from heating a binary solution of Cu nanoclusters and Ag nanoparticles ($T=145$ °C, $t_h=1.5$ hr); (D) Ag nanoparticles. (All particles are capped with decanethiolate monolayers). (E-F): TEM micrographs for samples from binary solutions of Au + Cu²⁺ absent with reducing agent and Au + Cu²⁺ present with reducing agent systems.

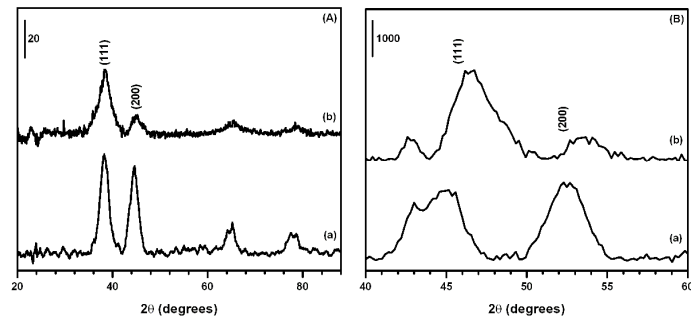


Figure S5. Wide angle XRD patterns obtained in house (A) and at a synchrotron radiation source (x-ray energy: 6.9 keV) (B). (A) (a) $\text{Au}_{66}\text{Cu}_{34}$ nanocubes (i.e., sample in Figure 1); (b) $\text{Au}_{34}\text{Cu}_{66}$ nanoparticles (i.e., sample in Figure S8a). (B) (a) the initial $\text{Au}_{66}\text{Cu}_{34}$ nanocubes/Si; (b) after in situ heating at 260 °C for 10 min.

Reference

1. Maye, M. M.; Zheng, W. X.; Leibowitz, F. L.; Ly, N. K.; Zhong, C. J. *Langmuir* **2000**, *16*, 490.
2. Buffat, P.; Borel, J. P. *Phys. Rev. A* **1976**, *13*, 2287.
3. Schadt, M. J.; Cheung, W.; Luo, J.; Zhong, C. J. *Chem. Mater.* **2006**, *18*, 5147.
4. Mott, D.; Yin, J.; Engelhard, M.; Loukrakpam, R.; Chang, P. G.; Bae, I-T.; Das, N. Chandra.; Wang, C.; Luo, J.; Zhong, C. J. *Chem. Mater.* **2010**, *22*, 261.
5. <http://en.wikipedia.org/wiki/Platinum>
6. Murr, L. E.; Cohen, M. *Interfacial phenomena in metals and alloys*. Addison–Wesley, Reading, MA, **1975**, 101.